AGU PUBLICATIONS

JGR

Journal of Geophysical Research: Atmospheres

RESEARCH ARTICLE
10.1002/2015JD023930

Key Points:
- We simulate the relative contribution of local and distant sources of surface ozone
- Ozone attributed to the model domain boundary is playing an increasingly important role
- Photochemical lifetime of ozone is lengthening because two primary gas phase sinks are decreasing

Supporting Information:
- Figures S1–S15

Correspondence to:
D. L. Goldberg,
dgoldb@atmos.umd.edu

Citation:
Goldberg, D. L., T. P. Vinciguerra, K. M. Hosley, C. P. Loughner, T. P. Canty, R. J. Salawitch, and R. R. Dickerson (2015), Evidence for an increase in the ozone photochemical lifetime in the eastern United States using a regional air quality model, *J. Geophys. Res. Atmos.*, *120*, 12,778–12,793, doi:10.1002/2015JD023930.

Received 14 JUL 2015
Accepted 24 NOV 2015
Accepted article online 27 NOV 2015
Published online 22 DEC 2015
Corrected 23 MAR 2016

This article was corrected on 23 MAR 2016. See the end of the full text for details.

Evidence for an increase in the ozone photochemical lifetime in the eastern United States using a regional air quality model

Daniel L. Goldberg[1], Timothy P. Vinciguerra[2], Kyle M. Hosley[3], Christopher P. Loughner[4], Timothy P. Canty[1], Ross J. Salawitch[1,4,5], and Russell R. Dickerson[1,4,5]

[1]Department of Atmospheric and Oceanic Science, University of Maryland, College Park, Maryland, USA, [2]Department of Chemical and Biomolecular Engineering, University of Maryland, College Park, Maryland, USA, [3]Department of Atmospheric and Oceanic Sciences, University of Wisconsin-Madison, Madison, Wisconsin, USA, [4]Earth System Science Interdisciplinary Center, University of Maryland, College Park, Maryland, USA, [5]Department of Chemistry and Biochemistry, University of Maryland, College Park, Maryland, USA

Abstract Measures to control surface ozone rely on quantifying production attributable to local versus regional (upwind) emissions. Here we simulate the relative contribution of local (i.e., within a particular state) and regional sources of surface ozone in the eastern United States (66–94°W longitude) for July 2002, 2011, and 2018 using the Comprehensive Air-quality Model with Extensions (CAMx). To determine how emissions and chemistry within the domain affect the production, loss, lifetime, and transport of trace gases, we initialize our model with identical boundary conditions in each simulation. We find that the photochemical lifetime of ozone has increased as emissions have decreased. The contribution of ozone from outside the domain (boundary condition ozone, BC_{O3}) to local surface mixing ratios increases in an absolute sense by 1–2 ppbv between 2002 and 2018 due to the longer lifetime of ozone. The photochemical lifetime of ozone lengthens because the two primary gas phase sinks for odd oxygen ($O_x \approx NO_2 + O_3$)—attack by hydroperoxyl radicals (HO_2) on ozone and formation of nitrate—weaken with decreasing pollutant emissions. The relative role of BC_{O3} will also increase. For example, BC_{O3} represents 34.5%, 38.8%, and 43.6% of surface ozone in the Baltimore, MD, region during July 2002, 2011, and 2018 means, respectively. This unintended consequence of air quality regulation impacts attainment of the National Ambient Air Quality Standard for surface ozone because the spatial and temporal scales of photochemical smog increase; the influence of pollutants transported between states and into the eastern U.S. will likely play a greater role in the future.

1. Introduction

Tropospheric ozone, in high enough concentrations, causes premature aging of the lungs [*Bell et al.*, 2004] and stunts the growth of plants [*Sandermann*, 1996]. To protect human health and agriculture, the Environmental Protection Agency (EPA) had limited ambient ozone to an 8 h daily maximum mixing ratio of 75 parts per billion by volume (ppbv) [*Environmental Protection Agency* (*EPA*), 2012]. On 1 October 2015, while this paper was under review, EPA revised the ozone National Ambient Air Quality Standard (NAAQS) to a 8 h daily maximum of 70 ppbv [*EPA*, 2015a]. Our paper will refer to the 75 ppbv standard, since this is the limit in effect at the time the research was conducted. Several health studies show deleterious effects from ozone even at low concentrations [*Bell et al.*, 2006; *Jerrett et al.*, 2009; *Anenberg et al.*, 2010; *Fann et al.*, 2011].

In the United States, surface ozone concentrations began to rise in the 1950s peaking in the 1980s [*Vingarzan*, 2004; *Oltmans et al.*, 2006]. Surface ozone concentrations have since declined with the most substantial decreases in the last decade [*Fiore et al.*, 1998; *Lin et al.*, 2001; *Vingarzan*, 2004; *Oltmans et al.*, 2006; *Oltmans et al.*, 2013] in response to emission reduction strategies of ozone precursors [*He et al.*, 2013; *Loughner et al.*, 2014; *Sickles and Shadwick*, 2015] as required by the Clean Air Act [*EPA*, 2014a]. For example, in 2002, the highest ozone design value—a weighted 3 year average of the fourth highest annual 8 h maximum ozone mixing ratio—for the Baltimore, Maryland, nonattainment region was 104.0 ppbv. In 2011, the highest value ozone design value for the same region decreased to 90.0 ppbv. Urban locations in the eastern United States have seen similar surface ozone reductions during the worst air quality days [*EPA*, 2012].

While many urban and suburban locations in the United States have undergone recent decreases in surface ozone concentrations, rural locations in the western United States have experienced increases [*Jaffe and Ray*, 2007]

especially in spring [*Cooper et al.*, 2010, 2012]. Some monitors in urban city centers have also seen increases in surface ozone, presumably due to less titration of ozone by local NO_x emissions [*Simon et al.*, 2015]. At monitors situated along the rural western North American coastline, mean annual observed ozone has been increasing at a rate of 0.34 ppbv/yr since the 1980s [*Parrish et al.*, 2009]. *Cooper et al.* [2012] reported an increase of ozone in the free troposphere during springtime of 0.41 ppbv/yr from 1995 to 2011 at rural sites in western North America. Between 1987 and 2007, a similar positive trend of 0.31 ppbv/yr was reported at the Mace Head observatory located at the westernmost coast of Ireland [*Derwent et al.*, 2007]. While ozone mixing ratios at Mace Head have plateaued in the late 2000s, there is no indication of stabilization at rural western North American coastline monitoring sites [*Parrish et al.*, 2009]. The increases of surface ozone in rural locations of western North America and western Europe may be the result of a growth in the global background mixing ratio of ozone [*Lin et al.*, 2000].

The fraction of ozone present in a given area not attributed to anthropogenic sources of regional origin is referred to as background ozone [*Vingarzan*, 2004]. A majority of background ozone can be attributed to uncontrollable sources such as stratospheric intrusions [*Langford et al.*, 2012; *Lin et al.*, 2012a], wildfires [*Val Martin et al.*, 2006], soil NO_x emissions [*Hudman et al.*, 2012; *Vinken et al.*, 2014], and lightning [*Allen et al.*, 2012]. The remaining portion is attributed to long-range transport of ozone of anthropogenic origin. The influence of Asian anthropogenic emissions can be a meaningful contributor to North American ozone mixing ratios, especially in the elevated terrain of western North America [*Jacob et al.*, 1999; *Lin et al.*, 2000; *Zhang et al.*, 2008; *Cooper et al.*, 2010; *Lin et al.*, 2012b; *Zhang et al.*, 2014a; *Gratz et al.*, 2015]. Similarly, states west of the Mississippi River can be meaningful contributors to ozone pollution in the eastern United States [*EPA*, 2015b]. As a whole, background ozone can represent between 15 and 50 ppbv of the mean surface ozone in North America [*Zhang et al.*, 2011; *Emery et al.*, 2012; *Fiore et al.*, 2014; *Lefohn et al.*, 2014; *Dolwick et al.*, 2015; *Baker et al.*, 2015].

Variations in tropospheric composition can alter the photochemical lifetime of ozone. On a global scale, the lifetime of tropospheric ozone is ~22 days [*Stevenson et al.*, 2006] calculated for the year 2000. The lifetime of ozone near the surface can be substantially shorter [*Jacob*, 2000]. *Lamarque et al.* [2005] report that the global ozone lifetime has decreased by 30% since the 1930s in response to anthropogenic emissions of NO_x and volatile organic compounds (VOCs). *Stevenson et al.* [2006] predicts mean ozone lifetime, on a global scale, will decrease by 10% between 2000 and 2030 as global emissions of anthropogenic NO_x and VOCs continue to increase. *Zhang et al.* [2014b] suggest that as stratospheric ozone recovers, tropospheric photolysis rates—including those that produce HO_x—will decrease, yielding a small increase in the tropospheric ozone lifetime assuming emissions remain constant. A limitation of these studies is that they were performed on global scale.

2. Methods

We use observations and the Comprehensive Air-quality Model with Extensions (CAMx) version 6.10 (also used by *EPA* [2015b]) with ozone source apportionment at a high spatial and temporal resolution to quantify the role of the long-range transport and regional anthropogenic emissions on total surface ozone mixing ratios in the eastern United States. In this study, we make extensive use of a quantity called boundary ozone (BC_{O3}): the sum of ozone transported across the four boundaries of our eastern United States modeling domain plus ozone formed from precursors transported across these boundaries; for this reason BC_{O3} is regional in nature. We use BC_{O3} as a reactive tracer to determine how the photochemical lifetime of ozone changes as anthropogenic NO_x and VOC emissions in the eastern United States decrease.

Our study focuses on three monthlong simulations of July. The baseline simulation is conducted for July 2011, using emissions and meteorological fields prepared for this summer. We also present simulations conducted using July 2011 meteorology and retrospective emissions from July 2002, and conducted using July 2011 meteorology and projected emissions for July 2018. The simulations for three Julys, using identical meteorological fields, were used to assess how the relative influence of local emissions and BC_{O3} on surface ozone in the eastern United States evolves, over time, due to changes in anthropogenic emissions.

2.1. Meteorological Model

Weather and Research Forecast (WRF) v3.4 was used to simulate the meteorology [*EPA*, 2014b] for this modeling study [*Skamarock et al.*, 2008]. The WRF model domain encompasses the Continental United States (CONUS) at a horizontal resolution of 12 km with 35 vertical levels from the surface to 50 millibars (mbar). The 12 km

North American Model (NAM) analysis provided by the National Climate Data Center (NCDC) was used for the WRF initial and outermost lateral boundary conditions. When NAM data were unavailable, the 40 km Eta Data Assimilation System analyses from the National Center for Atmospheric Research were used. Data were quality controlled and compared to observations, showing excellent agreement [*EPA*, 2014b]. The Group for High-Resolution Sea Surface Temperatures provided sea surface temperatures (SSTs) at 1 km resolution [*Stammer et al*., 2003]. High-resolution SSTs are critical for warm, shallow, coastal waters that influence the strength of bay and sea breezes. The WRF model was reinitialized every 5 days for the 2011 calendar year and run in 132 h increments; the first 12 h of each simulation was used for spin-up of the model meteorology. The WRF simulation was conducted offline. Meteorological data were fed to CAMx v6.10 at hourly intervals.

2.2. Emissions Processing Model

Anthropogenic emissions input files for CAMx v6.10 were created with the Sparse Matrix Operator Kernel Emissions modeling system [*Houyoux and Vukovich*, 1999] and converted to CAMx-ready format through the "cmaq2camx" preprocessor. We use version 1 of the 2011 National Emissions Inventory (NEI) as compiled by EPA for the baseline simulation [*EPA*, 2014c]. Mobile emissions estimates from cars, trucks, and motorcycles were computed with the Motor Vehicle Emission Simulator 2010b (MOVES2010) [*Kota et al*., 2012]. Point sources were vertically distributed based on the meteorology, stack height, as well as the temperature and velocity of pollutants exiting the stacks. Emission estimates for a hypothetical 2002 scenario using 2011 meteorology were made using the 2002 NEI. The Mid-Atlantic Regional Air Management Association (MARAMA) has provided anthropogenic emission projections for July 2018 based upon EPA recommendations [*EPA*, 2014c]. Emissions for the July 2002 and 2018 model simulations were based on meteorology from July 2011. Biogenic emissions were calculated using Biogenic Emissions Inventory System (BEIS) version 3.14 [*Pouliot and Pierce*, 2009] and were identical in each of the three model simulations.

2.3. Global Chemistry Models

The boundary conditions were initialized using the GEOS-Chem v8-03-02 global chemistry model [*Bey et al*., 2001] at a horizontal resolution of 2.5° × 2.0°. The "geos2cmaq" preprocessor [*Henderson et al*., 2014] assigns the value of the closest global model grid point to each boundary grid cell of the 12 km regional model. Boundary condition files were converted to CAMx-ready files using the cmaq2camx preprocessor [*Ramboll Environ*, 2014]. *Henderson et al*. [2014] analyzed the accuracy of ozone boundary conditions for a CONUS model domain using Ozone Monitoring Instrument (OMI) and TES; they found good agreement of ozone in the middle and upper troposphere (above 700 mbar) during the month of August 2006–2010 and a consistent underestimation closer to surface (below 700 mbar) during the same time period. Furthermore, *Fiore et al*. [2014] showed that observed midtropospheric ozone from the TES and OMI satellites in rural locations at our model domain boundary agreed to within 5 ppbv in GEOS-Chem, at a 2 × 2.5° resolution, during the summer of 2006. We also describe a sensitivity study in which we use a 2.5° × 1.9° Model for OZone and Related chemical Tracers version 4 (MOZART-4) simulation [*Emmons et al*., 2010] to initialize trace gases along the CAMx lateral boundaries. The "mozart2camx" preprocessor [*Ramboll Environ*, 2014] interpolates the global model data to the closest 12 km regional model grid cell. A plot of mean July 2011 ozone for the eastern United States from MOZART-4 is provided in the supporting information (Figure S1).

2.4. Regional Air Quality Model

We use CAMx version 6.10 for this study. We simulate air pollutant mixing ratios from 26 May 2011 to 31 August 2011 with a focus on July 2011. Horizontal resolution is 12 km and covers the domain depicted in Figure 1. Fine-scale features associated with cumulus cloud venting and bay and sea breeze effects [*Loughner et al*., 2011; *Goldberg et al*., 2014] cannot be captured with a 12 km horizontal grid, but the general behavior of ozone is reproduced with reasonable fidelity [*Goldberg et al*., 2014]. All 35 vertical layers from the WRF simulation were passed to the CAMx regional model. Horizontal and vertical advections were calculated using the Piecewise Parabolic Method [*Colella and Woodward*, 1984]. Vertical eddy diffusion was calculated using K_z theory [*O'Brien*, 1970]. We use the Carbon Bond 05 (CB05) gas phase chemistry with Coarse-Fine (CF) aerosols [*Yarwood et al*., 2005] calculated with the Euler backward iterative (EBI) solver. Photolysis rates were calculated using the tropospheric ultraviolet-visible radiation model by the discrete-ordinates method; ozone columns used in the photolysis rate calculations were based on retrievals from the Ozone Monitoring Instrument (OMI) satellite. Model simulations started on 16 May 2011 using initial conditions provided by the

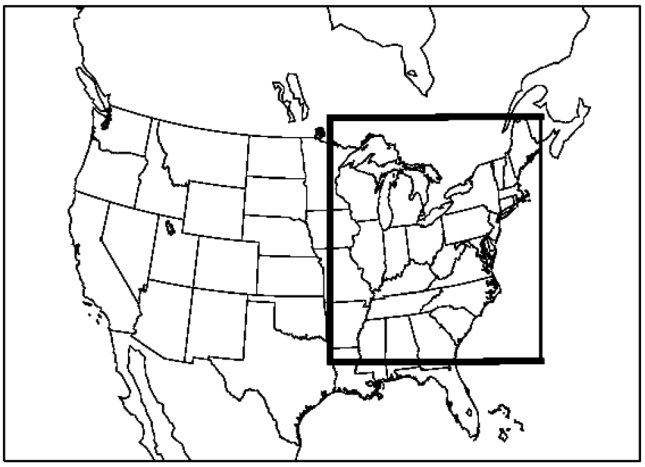

Figure 1. CAMx v6.10 model domain as denoted by the dark black line, 12 km horizontal resolution.

MOZART-4 global model; we allow for 10 days of spin-up of CAMx. After the 10 day period, less than 0.1% of the initial conditions remain in the model domain. The simulation begins on 26 May, the first ozone exceedance day in Maryland during 2011.

The Ozone Source Apportionment Technology (OSAT) is an add-on software package for CAMx [*Ramboll Environ*, 2014], which allocates ozone at receptor source locations to upwind source regions (i.e., states, cities, etc.) and types (mobile, point, etc.). *Collet et al.* [2014] document how OSAT differs from a zero-out method—a scenario in which anthropogenic emissions from a single region or sector are completely eliminated. Particularly useful for this study, OSAT tracked boundary conditions and initial conditions as separate group categories. We also use the Chemical Process Analysis (CPA) probing tool to calculate production and loss rates of ozone and some of its precursors. A detailed description of the OSAT and CPA software can be found in the CAMx version 6.10 User's Manual [*Ramboll Environ*, 2014].

2.5. Model Limitations

While biogenic emissions for this study were calculated using BEIS v3.14, *Canty et al.* [2015] show better agreement with the Model of Emissions of Gases and Aerosols from Nature (MEGAN) v2.1 model [*Guenther et al.*, 2012]. Isoprene emissions are larger in the MEGAN model when compared to BEIS [*Warneke et al.*, 2010; *Carlton and Baker*, 2011]. Several studies also suggest an overestimation of NO_x emissions from mobile sources [*Fujita et al.*, 2012; *Anderson et al.*, 2014] using MOVES2010 [*Kota et al.*, 2012]. Furthermore, the Carbon Bond 6 Revision 2 (CB6r2) gas phase chemistry has been released recently [*Hildebrandt-Ruiz and Yarwood*, 2013]; this updated mechanism more explicitly represents alkyl nitrates in regional air quality models: an improvement over CB05 [*Canty et al.*, 2015]. CB6r2 calculates a shorter lifetime of alkyl nitrates and faster recycling of NO_x. This may improve the simulation of ozone attributed to long-range sources. *Canty et al.* [2015] concluded regional air quality models underestimate the importance of interstate transport of NO_x; therefore, the actual ozone mixing ratios attributed to upwind states and the boundary may be increased with respect to values found in our baseline simulation.

3. Results and Discussion

3.1. Observations of Ozone

Atmospheric conditions in the eastern United States during July 2011 were conducive for poor air quality: hot temperatures with generally clear skies and a persistent subsidence inversion [*Loughner et al.*, 2014]. Maximum 8 h surface ozone within the state of Maryland and maximum afternoon temperature at the Baltimore-Washington International (BWI) airport during July 2011 are shown in Figure 2. Twenty-nine days at BWI had high temperatures above 30°C; the monthly temperature anomaly was +2.9°C compared to 1980–2010 climatology [*National Climate Data Center* (*NCDC*), 2015]. Many of the days in July 2011 also had stagnant or southwesterly winds and clear skies, maximizing photochemical ozone production [*NCDC*, 2015]. Correspondingly, there were 17 days during July 2011 when 8 h maximum surface ozone exceeded the 75 ppbv NAAQS in the state of Maryland [*Loughner et al.*, 2014].

Despite consistently exceeding the NAAQS during July 2011, surface ozone in the Baltimore-Washington metropolitan area has seen large decreases since the 1970s. In Figure 3, we plot daytime averages of carbon monoxide (CO), nitrogen dioxide (NO_2), and top and bottom third of the distribution of daytime ozone (O_3) surface mixing ratios in the Baltimore-Washington metropolitan area since 1972, a 40 year record.

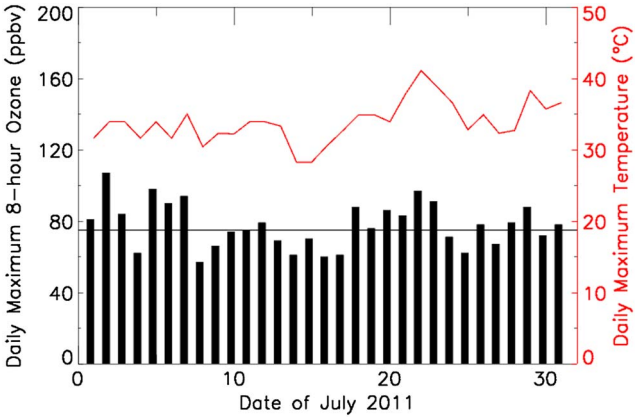

Figure 2. Maximum 8 h ozone mixing ratios (ppbv) in the Baltimore nonattainment area during each July 2011 date (black bar plots, left axis) and plot of maximum daily temperature (°C) at the Baltimore-Washington International airport (red curve, right axis).

Instruments used to measure NO_2 also respond quantitatively to peroxyacyl nitrate, alkyl nitrates, and other reactive nitrogen species [*Fehsenfeld et al.*, 1987], but are suitable for trends. Since the early 1970s, CO mixing ratios have decreased by almost 2 orders of magnitude and NO_2 mixing ratios have declined by 1 order of magnitude. Due to the nonlinearities in surface ozone production, ozone mixing ratios have declined at a slower rate. There has been a -0.38 ± 0.06 ppbv yr^{-1} decline in the top third of monthly daytime ozone during the ozone season (April to October). Three federal regulatory measures, labeled in Figure 3, have contributed to the decrease in surface ozone over the past four decades: mandatory catalytic converters in automobiles, reformulated gasoline, and selective catalytic reduction scrubbing of NO_x from power plants.

While the Baltimore-Washington metropolitan area has experienced a steady decline in the highest daytime ozone levels, the bottom third of monthly daytime ozone levels during the ozone season have been steadily rising at a rate of $+0.37 \pm 0.04$ ppbv yr^{-1}. The rise of the bottom third of the ozone distribution suggests background ozone in the Baltimore-Washington metropolitan region could be rising at a rate similar to that observed in the western United States [*Parrish et al.*, 2009]. This is similar to what is shown by *Cooper et al.* [2012]; they demonstrate a statistically significant positive trend in the 5th percentile of surface ozone in Baltimore-Washington metropolitan region during spring and a weak positive trend during summer. They hypothesize that the eastern United States could be affected by an increase in the global background ozone.

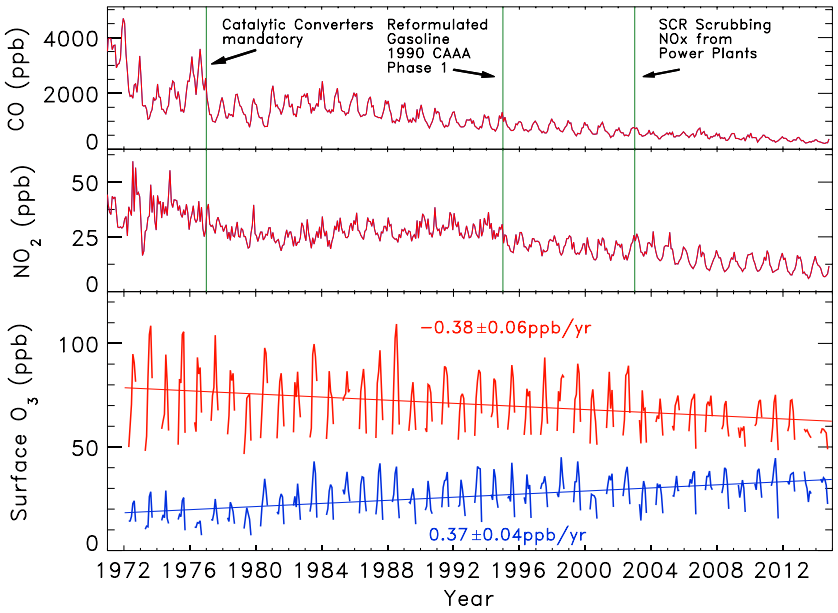

Figure 3. Observations at the surface of (top) CO, (middle) NO_2 and the (bottom) top third of the distribution of ozone observations (red curve) and bottom third (blue curve) from EPA monitoring sites in MD, DC, and Northern VA. The CO and NO_2 data are monthly averages. The ozone data are monthly daytime averages during the ozone season (April–October); colored solid lines indicate a linear fit to each of the data distributions. Vertical lines indicate the enactment of federal regulations that led to declines in CO and NO_2.

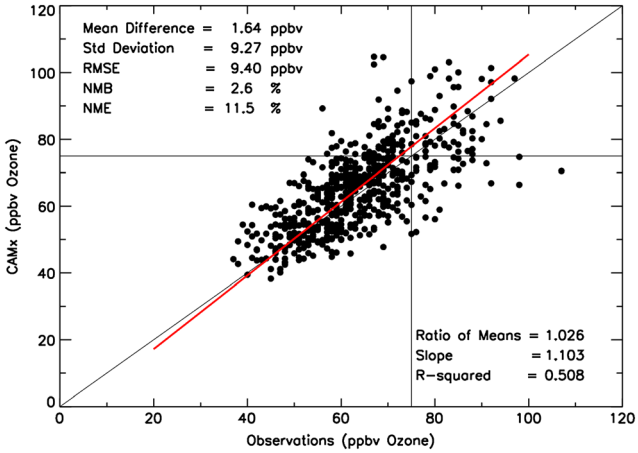

Figure 4. Observed 8 h maximum ozone mixing ratios (ppbv) at the surface from the Maryland Department of the Environment monitoring network versus modeled 8 h maximum ozone mixing ratios using CAMx version 6.10, during July 2011.

In this study, we expand upon the hypothesis from *Cooper et al.* [2012] by examining how reductions of anthropogenic NO_x and VOC emissions in the eastern United States could be responsible for a rise in the background ozone.

It is also possible that the rise in the bottom third of the ozone distribution is due, in part, to less titration of ozone by NO_x, particularly for heavily polluted areas such as urban centers [*Simon et al.*, 2015]. If the decline in titration of ozone by NO_x were truly responsible for a rise in the lower third of the ozone distribution, then the extremely high prior abundance of NO_2 would have been harmful to human health [*Samoli et al.*, 2006]. Quantification of the two separate drivers of the upward trend in the bottom third ozone (i.e., rising background ozone coupled with rising influence of background ozone; less titration of ozone to very low levels) will be the subject of a future study conducted by our group.

While policy for surface ozone in the U.S. is presently focused on daily 8 h maximum that is reflected by the upper third of the surface ozone distribution, the impact of ozone on trees, plants, and ecosystems is often assessed using weighted indices designed to reflect the cumulative exposures to ozone experienced during the growing season [*Paoletti and Manning*, 2007]. Furthermore, *Bell et al.* [2006] reported increased risk of premature mortality for even low levels of surface ozone. The narrowing of the surface ozone distribution, reflected by the convergence of the upper and lower thirds illustrated in Figure 3, suggests that improvement in air quality is overstated if based solely on the decline in daily 8 h maximum.

3.2. Using OSAT to Determine the Role of Boundary Ozone

We simulate ozone mixing ratios during July 2011 in the Baltimore, Maryland, region using CAMx v6.10 with OSAT. Observations from the Maryland Department of the Environment (MDE) network and Clean Air Status and Trends NETwork (CASTNET) were used to evaluate CAMx performance. Figure 4 shows observed 8 h maximum ozone mixing ratios from the MDE monitoring network versus the same quantity from CAMx. There is a mean monthly bias of +1.64 ppbv in predicting July 2011 8 h maximum surface ozone in Maryland. We also display the standard deviation, root-mean-square error, normalized mean bias, and normalized mean error. When comparing modeled July 2011 8 h maximum surface ozone to CASTNET sites, which are located in more rural locations, Figure S2, there is a +7.00 ppbv bias.

We now use OSAT to determine which source regions are responsible for total surface ozone mixing ratios during July 2011. Figure 5 shows the source apportionment of midafternoon surface ozone in the Baltimore, Maryland, region for the July 2011 mean and three of the observed worst air quality days during the month: 2 July, 7 July, and 22 July. We define the Baltimore region as a 72×96 km rectangular box inclusive of the entire metropolitan region. Ozone attributed to the model domain boundary (BC_{O3}) plays an important role in Maryland's midafternoon ozone concentration. For the July 2011 average, 26.8 ppbv of surface ozone, or 38.8%, of the total mixing ratio in the Baltimore, Maryland, region can be attributed to BC_{O3}. An *EPA* [2015b] modeling study using a CONUS domain during the summer of 2011 estimates boundary contribution during poor air quality days in Maryland to be 16–19 ppbv. Another 27.3 ppbv, or 39.6%, is attributed to emissions of ozone precursors within the model domain boundary, but excluding the state of Maryland. Finally, 14.9 ppbv, or 21.6%, of surface ozone is attributed to the emissions of ozone precursors from sources within the state of Maryland.

The portion of ozone in the Baltimore region attributed to emission sources outside Maryland's borders but within the eastern United States model domain (blue bar) exhibits the most day-to-day variation. On 2 July 2011, a day

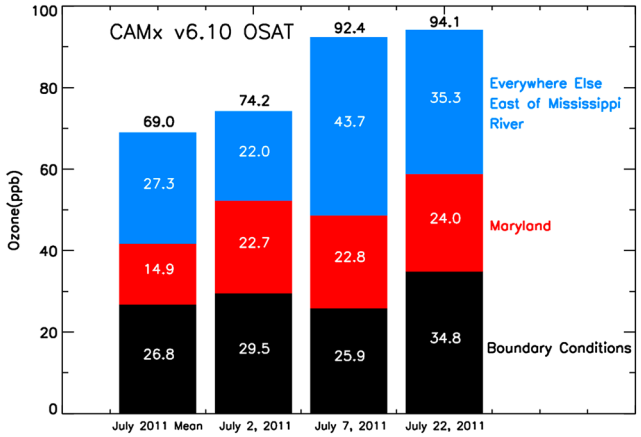

Figure 5. Mean ozone source apportionment (ppbv) at the surface at 2 P.M. EDT in a 72 × 96 km rectangular box encompassing Baltimore, MD, for the July 2011 mean and the three observed worst air quality days during the month: 2 July, 7 July, and 21 July. The black bars represent the contribution from beyond the model domain boundary, the red bars represent the contribution from the state of Maryland, and the blue bars represent the contribution from all other areas within the model domain.

with stagnant winds classified as a local pollution episode, the portion of ozone from within the state's border was of similar magnitude to the portion of ozone attributed to outside of Maryland's borders: 22.7 ppbv versus 22.0 ppbv. On 7 July 2011, a day with strong westerly winds, the portion of ozone attributed to sources outside the state is 43.7 ppb, compared to 27.3 ppb during the July mean. These simulations suggest that the magnitude and extent of the poor air quality during the worst air quality days, the ones that qualify areas for nonattainment status, are not determined only by local sources but instead are a combination of local production and high ozone anomalies advected downwind.

The 22 July is a case study in which ozone anomalies extended beyond our model domain. While in-domain sources were still responsible for the majority of the ozone on this day, we also see an increased influence from the boundaries. On 22 July, the amount of ozone attributed to BC_{O3} is increased 8.0 ppbv over the mean BC_{O3} mixing ratio. This may indicate that high ozone anomalies beyond the model domain's border are further enhancing the high mixing ratios at the surface in Maryland.

Since BC_{O3} can be a significant portion of total surface ozone, we examine the four model domain boundaries to determine which boundaries are influencing mid-Atlantic surface mixing ratios the most. Figure 6 shows monthly averaged midafternoon ozone mixing ratios attributed to each model boundary; these are not total mixing ratios but contributions from each of the four edges of the domain. The western

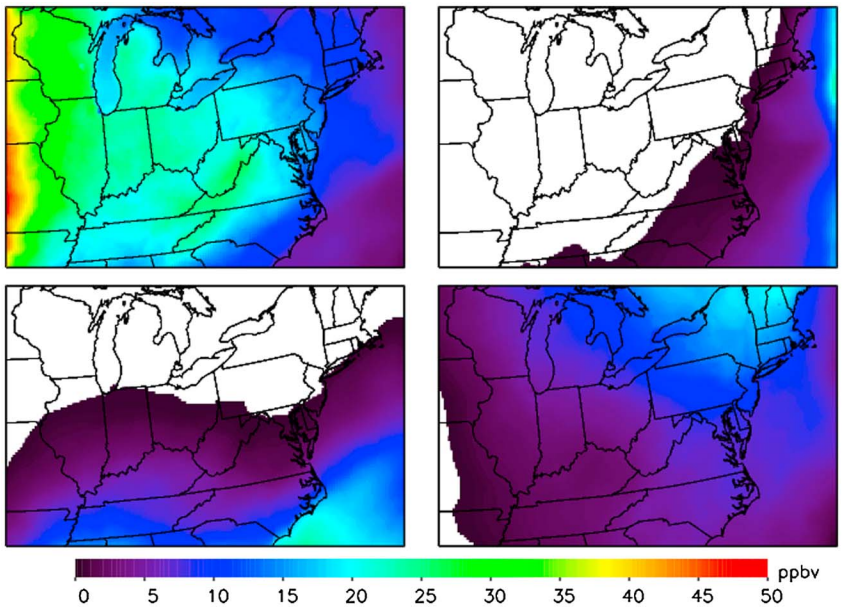

Figure 6. Ozone mixing ratios (ppbv) at the surface attributed to the four cardinal direction boundaries: (top left) west, (top right) east, (bottom left) south, and (bottom right) north, averaged for the entire month of July at 2 P.M. EDT.

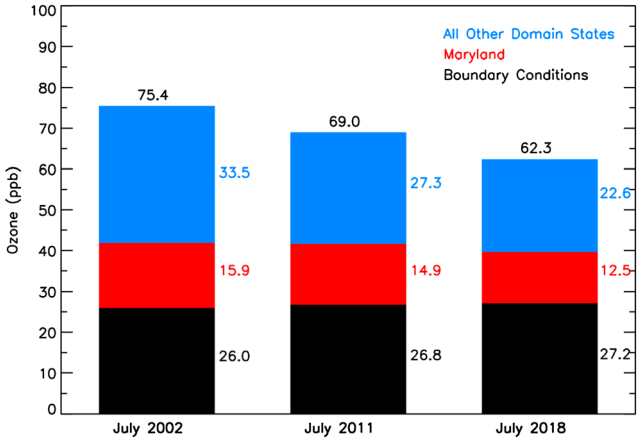

Figure 7. Mean ozone source apportionment (ppbv) at the surface at 2 P.M. EDT in a 72 × 96 km rectangular box encompassing the Baltimore, MD, region for 7 July 2002, 2011, and 2018. Input emissions were calculated using the NEI for the respective year and 2011 meteorology. The black bars represent the contribution from beyond the model domain boundary, the red bars represent the contribution from the state of Maryland, and other color represents the contribution from various regions within the model domain.

model domain is the primary contributor to BC_{O3} in the majority of the model domain, including Maryland. Westerly winds are the dominant flow pattern in our region of study, advecting trace gases primarily from the western boundary (94°W longitude) to the east in the model domain. Meridional flow from strong cyclones or anticyclones can perturb the dominant westerly flow, but these features are not persistent enough to modify the mean zonal flow. Mixing ratios of ozone from the western model domain boundary exceed 20 ppbv at the surface in most areas. The western model boundary has the least influence on surface ozone in New York, New England, and parts of Canada, where the northern boundary is the primary contributor. Ozone initialized at the southern and eastern boundaries has little effect on Maryland and much of the model domain during July 2011.

3.3. Role of the Boundary Ozone in Model Simulations of Future Years

Surface ozone concentrations during the worst air quality days in the eastern United States are projected to decrease in next decade in response to pollution control policies and market-based switches to cleaner technology. The 2018 Design Value for the most polluted monitor in the Baltimore metropolitan area—as calculated by EPA guidance [*EPA*, 2014d] using our CAMx simulation—is 79.0 ppbv, down from the observed 2011 Design Value of 90.0 ppbv, a reduction of 12.2%. This leaves the Baltimore area in violation of the 2008 NAAQS [*EPA*, 2012] without further emission reduction strategies. We provide future state-by-state contribution to total surface ozone in the supporting information (Figure S3).

We now describe a CAMx sensitivity study in which trace gas mixing ratios at the boundary for the month of July 2002 and July 2018 remain at July 2011 mixing ratios; emissions of ozone precursors within the domain vary according to the respective year as described in section 2.2. Figure 7 shows the apportionment of surface ozone in the vicinity of Baltimore from various source regions in the midafternoon during July 2002, 2011, and 2018; all years use 2011 meteorology. In the 2002 scenario, contribution from outside the model domain is 34.5% of the total ozone and by 2018 the percentage increases to 43.6% in Baltimore. The same tendency for BC_{O3} to have an increasing role for surface ozone is applicable to other regions in the eastern United States, such as New York City, Atlanta, and Chicago, as shown in Table 1. Between 2002 and 2018 there is a definitive trend for contributions from within the model domain to lose influence on total ozone during the summer. Figure 7 also shows that BC_{O3} increases from 26.0 ppbv in 2002 to 27.2 ppbv in 2018, a +4.6% increase over 16 years, in the Baltimore metropolitan area. This increase is also seen in other urban areas in the eastern United States as shown in Table 2. We also show the same finding using CB6r2 gas phase chemistry (Figure S4) in the supplementary material.

Table 1. Percentage of Ozone Attributed to the Boundary at Each Receptor Location During the July Mean of 2002, 2011, and 2018[a]

Metropolitan Area	2002	2011	2018
New York, NY	37.0%	41.6%	45.3%
Philadelphia, PA	38.1%	42.7%	47.6%
Baltimore, MD	34.5%	38.8%	43.6%
Washington, DC	35.9%	41.0%	46.5%
Atlanta, GA	43.6%	49.0%	56.3%
Chicago, IL	45.9%	48.2%	52.0%

[a]Chicago is near the western boundary of our model domain, and results may be less reliable.

We attribute the increase in BC_{O3} to lower O_x ($O_x = O_3 + (NO_y - NO)$) loss

Table 2. Portion of Ozone (ppbv) Attributed to the Boundary at Each Receptor Location During the July Mean of 2002, 2011, and 2018

Metropolitan Area	2002	2011	2018
New York, NY	23.9	24.6	25.9
Philadelphia, PA	26.8	27.4	27.7
Baltimore, MD	26.0	26.8	27.2
Washington, DC	27.2	27.6	28.0
Atlanta, GA	30.1	30.6	31.1
Chicago, IL	26.9	28.7	29.6

rates in the future. Figure 8 shows that in 2002, O_x loss rates in Maryland were 1.5 ppbv per hour during the daytime (8 A.M. to 8 P.M. local time). In 2018, O_x loss rates over the same time frame are projected to be 1.2 ppbv per hour, a difference of −0.3 ppbv per hour. A reduction in O_x loss rates yields a longer lifetime of ozone in the troposphere.

Our analysis suggests two reasons why O_x loss rates decline in the future: decreased removal of ozone by HO_2 and decreased removal of NO_2 by oxidation to nitrate (NO_3^-). The $HO_2 + O_3$ reaction can be an important sink for ozone in nonurban, nonindustrial regions and especially at altitudes above the surface layer [*Wang et al.*, 1998]. Figure 9 shows a dichotomy between urban and rural regions; the highest mixing ratios of HO_2 are focused in the rural regions of the southeastern United States, while the lowest mixing ratios of HO_2 are \found in major metropolitan areas. Typical HO_2 mixing ratios in nonurban, nonindustrial locations (where NO_x mixing ratios are low, < 1 ppbv) can be an order of magnitude larger in rural areas than in urban regions due to isoprene oxidation [*Trainer et al.*, 1987]. In urban regions (where NO_x mixing ratios are high, >5 ppbv), mixing ratios of HO_2 are low because HO_2 readily reacts with high mixing ratios of NO to create NO_2 and OH, reducing the abundance of HO_2 and causing the $HO_2 + O_3$ reaction to be locally unimportant for the loss of ozone. Our modeled mixing ratios of mean HO_2 agree well with measurements from *Martinez et al.* [2003], as shown in the supporting information (Figures S5–S7).

Decreased removal of ozone via chemical reaction with HO_2 in nonurban, nonindustrial regions of the atmosphere is one reason why there is a decrease in O_x loss between July 2002 and 2018. Figure 9 shows

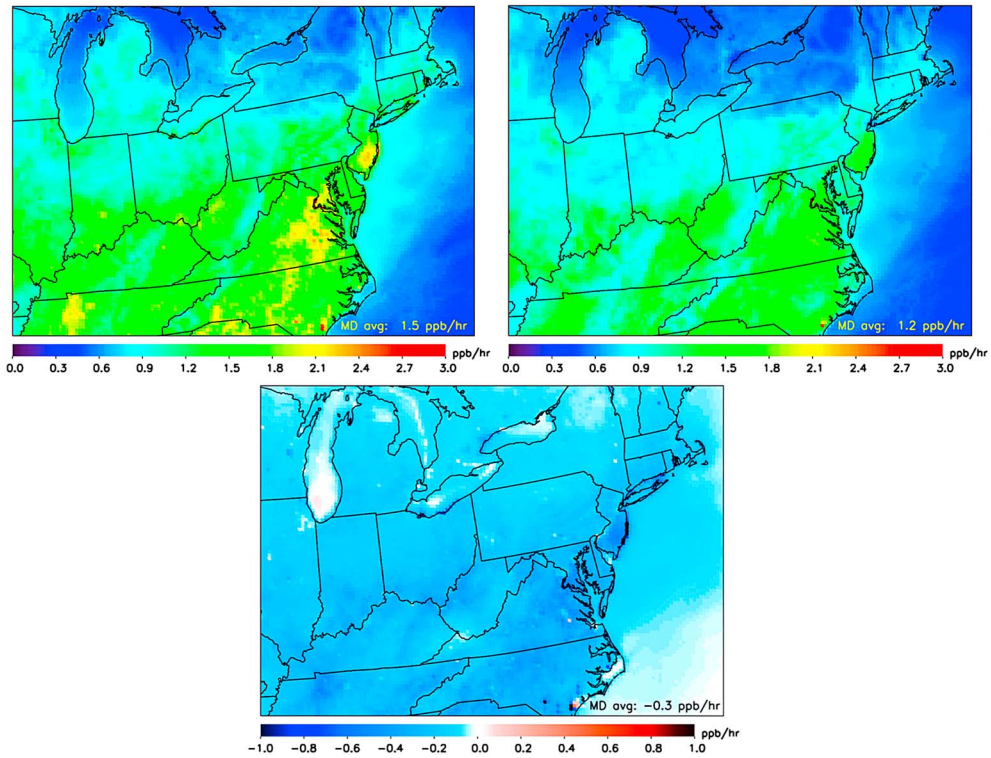

Figure 8. Mean daytime (8 A.M. to 8 P.M. local time) loss of O_x ($O_3 + [NO_y - NO]$) for (top left) July 2002, (top right) July 2018, and the (bottom) difference (July 2018 to July 2002) from the Chemical Process Analysis (CPA) probing tool in CAMx.

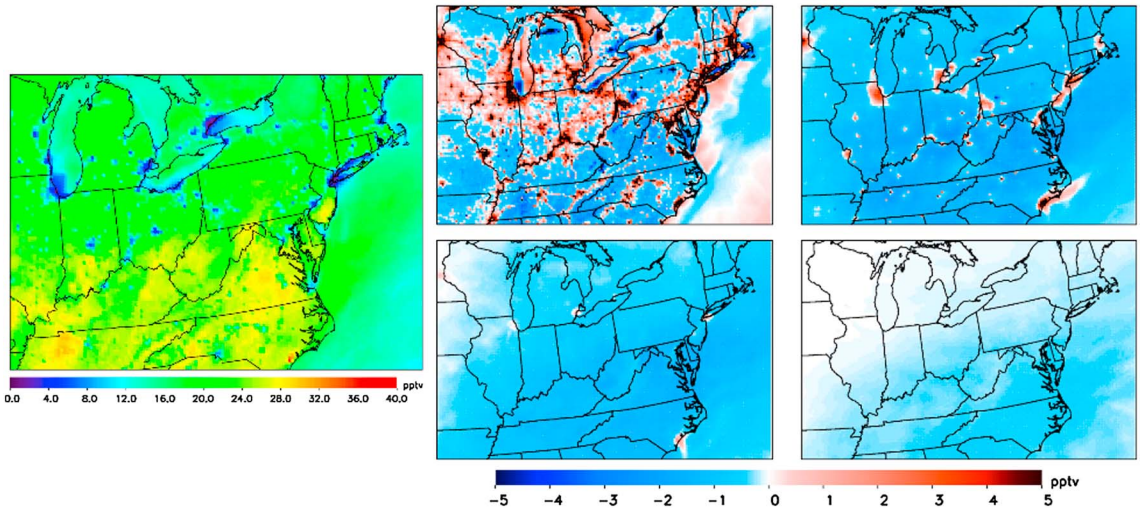

Figure 9. (left) Mean July 2011 daytime (7 A.M. to 7 P.M. local time) HO_2 mixing ratios (pptv). (right) Difference of mean HO_2 daytime (8 A.M. to 8 P.M. local time) mixing ratios (pptv) between July 2002 and July 2018: at the surface (top left), 1 km above the surface (top right), 2 km above the surface (bottom left), and 5 km above the surface (bottom right).

a plot of the difference in monthly mean HO_2 between July 2002 and 2018 for the eastern United States at the surface and three vertical layers (1, 2, and 5 km above the surface). Between 2002 and 2018, the CAMx simulation shows a 1–3 pptv decrease in HO_2 mixing ratios at the surface in nonurban, nonindustrial locations south and west of the mid-Atlantic. This area of the mid-Atlantic is particularly important because winds are usually from the southwest during the worst air quality episodes. Urban areas have higher future HO_2 mixing ratios due to less titration by the decreased NO_x emissions. Above the surface—especially at 1 and 2 km above the surface—the projected decrease in HO_2 is spatially uniform. Ozone above the surface layer is most affected by this decline in the abundance of HO_2. The mean change in ozone lifetime with respect to reaction with HO_2 at the surface, between 2002 and 2018, is modest: 9.21 days to 9.42 days. However, 1 km above the surface, the lifetime of ozone with respect to reaction with HO_2 increases from 8.98 days to 9.48 days. In the 2002 scenario, 11.1% of ozone is removed per day via reaction with HO_2, while in the 2018 scenario, 10.5% of ozone is removed per day via reaction with HO_2 (Table 3). Even though our model simulation has a 7 ppbv rural high bias in predicting ozone, the relative change in lifetime of ozone is insensitive to the absolute concentration of ozone (within 1 sigma).

The decreases in HO_2 above the surface layer and in rural regions are due to area wide decreases in anthropogenic emissions of NO_x and VOCs; biogenic emissions and meteorology remain identical between the two simulations. The primary sources and sinks of HO_2 are listed below [*Jacob*, 2000]:

Sources

$$RH + OH \xrightarrow{O_2} RO_2 + HO_2 \quad \text{(R1)}$$

$$RO_2 + NO \rightarrow RO + NO_2 \quad \text{(R2a)}$$

$$RO + O_2 \rightarrow R'CHO + HO_2 \quad \text{(R2b)}$$

$$RO + h\nu \xrightarrow{2O_2} 2HO_2 + R'O \quad \text{(R3)}$$

Sinks

$$HO_2 + HO_2 \rightarrow H_2O_2 + O_2 \quad \text{(R4)}$$

$$HO_2 + RO_2 \rightarrow ROOH + O_2 \quad \text{(R5)}$$

$$HO_2 + OH \rightarrow H_2O + O_2 \quad \text{(R6)}$$

Table 3. The Percentage (%) of Ozone Lost per Day Due To Two Changing Sinks of Ozone in July 2002 and July 2018, and the Change Between the 2 Years

Ozone Loss Mechanism	2002	2018	Δ
Loss by HO_2 per day	11.1%	10.5%	+0.6%
Loss by HNO_3 per day	5.2%	3.5%	+1.7%

The production of HO_2 is controlled by both VOC and NO_x emissions. Alkanes (RH) and carbonyls (R'CHO) can be direct sources of HO_2 via reactions 1 and 3. Decreased concentrations of alkanes and carbonyls will result in lower production of HO_2. NO_x emissions can also indirectly affect the HO_2 radical; lower concentrations of NO lead to slower production of HO_2 via reaction 2. The removal of HO_2 will also proceed more slowly, since the primary sink of HO_2 is the self-reaction (reaction 4). In the supporting information we show a plot of the difference of HO_2 between the 2002 simulation and a sensitivity experiment in which we keep NO_x emissions in 2018 identical to 2002. The decrease of HO_2 in rural areas and above the surface is smaller than the decrease shown in Figure 9. Therefore, we conclude that reductions in the emissions of VOCs as well as the nonlinearities associated with declining NO_x emissions are both responsible for the simulated decline in HO_2 that leads to an increase in the photochemical lifetime with respect to loss of tropospheric ozone.

The second explanation for the increase in the lifetime of ozone is less removal via daytime $NO_2 + OH$ reacting to form HNO_3 as well as nighttime hydrolysis of N_2O_5. At night, reaction between ozone and NO_2 can be a sink of ozone—during the daytime, this reaction results in NO_3 being quickly photolyzed back to NO_2. The reactions proceed as follows:

$$O_3 + NO_2 \rightarrow NO_3 + O_2 \quad \text{(R7)}$$

$$NO_3 + NO_2 + M \rightarrow N_2O_5 + M \quad \text{(R8)}$$

$$N_2O_5 + H_2O \xrightarrow{\text{aerosol}} 2\ HNO_3 \quad \text{(R9)}$$

As anthropogenic NO_x emissions decline, removal of ozone via $NO_2 + OH$ and N_2O_5 hydrolysis will decrease. This is normally a minor sink for ozone, but the change in NO_x between 2002 and 2018 is large enough to have a nontrivial effect. We show in the supporting information that HNO_3 deposition has decreased domain wide from 185 kg/km^2 month to 112 kg/km^2 month between July 2002 and 2018 (Figures S9 and S10); calculations using equation (1) show a change in lifetime of ozone with respect to loss from nitrate formation to increase from 19.2 days to 28.6 days (planetary boundary layer (PBL) = 1000 m, $[O_3]_{2002} = 43.1$ ppbv, $[O_3]_{2018} = 38.8$ ppbv). In the 2002 scenario, 5.2% of ozone is removed per day, while in the 2018 scenario, 3.5% of ozone is removed per day, as seen in Table 3.

$$\tau_{O_3} = \frac{[O_3]^{*}PBL_{depth}}{[HNO_3]_{deposition}} \quad (1)$$

Between these two explanations—less removal of ozone by HO_2 and by NO_2 through nitrate formation—we have accounted for the increase of the ozone lifetime. The change with respect to the HO_2 sink yields a +0.6% change per day, and the change with respect to the nitrate sink represents a +1.7% change per day. Taken together, this is a 2.3% per day increase in the lifetime of ozone. Typically, air parcels travel for 1 to 3 days in the model domain before reaching the East Coast of the United States—where our modeling study is focused. This yields a +4.6% change over a 2 day period, which reconciles the +4.6% change found in our modeling study. Table 4 and figures in the supporting information (Figures S11–S15) show changes in termination rates of HO_2 and HNO_3. In each case, termination rates have weakened yielding a longer lifetime of O_x.

Table 4. The Production and Loss Rates (ppbv/h) of Five Important Reactions During July 2002 and July 2018[a]

Chemical Process Analysis	2002	2018	Δ
HO_2 production	2.20	1.80	−0.40
HO_2 termination	1.60	1.30	−0.25
HNO_3 from $NO_2 + OH$	0.40	0.20	−0.20
HNO_3 from NO_3 + organics	0.03	0.01	−0.02
HNO_3 from N_2O_5 + water	0.11	0.02	−0.09

[a]HO_2 production, HO_2 termination, and $NO_2 + OH$ termination rates were calculated for the daytime mean (8 A.M.–8 P.M. local time). NO_3 + organics termination and N_2O_5 + water termination were calculated for the nighttime mean (8 P.M.–8 A.M.). The last column shows a difference between the 2002 and 2018 means.

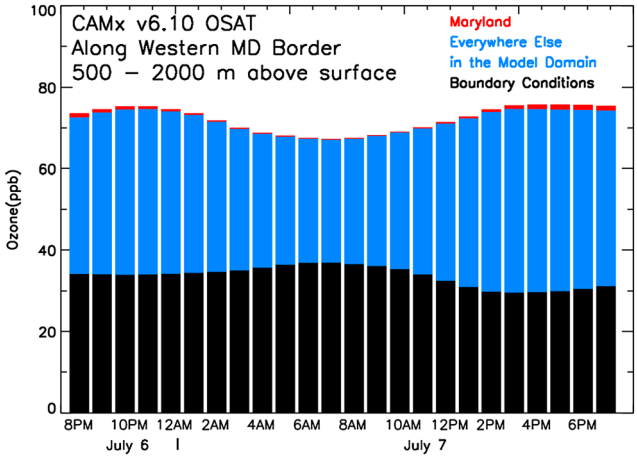

Figure 10. Ozone source apportionment (ppbv) between 500 and 2000 m above the surface in a 12 × 180 km "wall of cells" representing the western state border of Maryland during 7 July 2011, a day with westerly transport, confirmed by Hybrid Single-Particle Lagrangian Integrated Trajectory. The black bars represent the contribution from beyond the model domain boundary, the red bars represent the contribution from the state of Maryland, and other color represents the contribution from various regions within the model domain.

3.4. Role of Ozone Above the Surface

Ozone can also be tagged in individual plumes above the surface. Figure 10 depicts average hourly ozone source apportionment in an aloft plume 500–2000 m above ground level (agl) between 39° and 40°N along 78°W on 7 July 2011. The tagged plume was upwind of Maryland on 7 July: a day with large interstate transport as denoted in Figure 5. The ozone in the aloft plume is near 75 ppbv overnight and into the early morning. This high mixing ratio of ozone can mix down in the morning leading to rapid spikes when the nocturnal boundary layer breaks up. The diurnal cycle of total ozone aloft shows a much weaker daily cycle than during a day: a 10 ppbv change between the morning minimum and afternoon maximum. When total mixing ratios are at a minimum just after sunrise (7 A.M.), BC_{O3} is at a maximum.

We suggest the following conceptual model: Overnight, the ozone mixing ratio in the residual layer, 500–2000 m agl, decreases due to a lack of photochemical production. In contrast, ozone attributed to the boundary increases due to easier mixing from the free troposphere. At approximately 8 A.M. when the nocturnal temperature inversion breaks up, the previous day's residual layer mixes into the newly formed PBL, decreasing the portion attributed to the boundary but increasing the portion attributed to sources at or near the surface. At the same time, precursors from upwind states, which are essentially dormant overnight, can begin to react to photochemically produce ozone. In this scenario, much of the boundary ozone at the surface mixes down from aloft instead of being horizontally advected from the model domain boundary. Quantifying and verifying the ozone aloft is (500–2000 m agl) is of critical importance as these can affect peak daytime mixing ratios in downwind locations.

3.5. Initialization With Different Global Models

With the increased role of BC_{O3} in the past decade, the choice of boundary initialization has become more important. A sensitivity study [*Akritidis et al.*, 2013] using a 50 km × 50 km regional model showed that time invariant chemical boundary conditions do not capture the seasonal variability of ozone. Adding seasonal

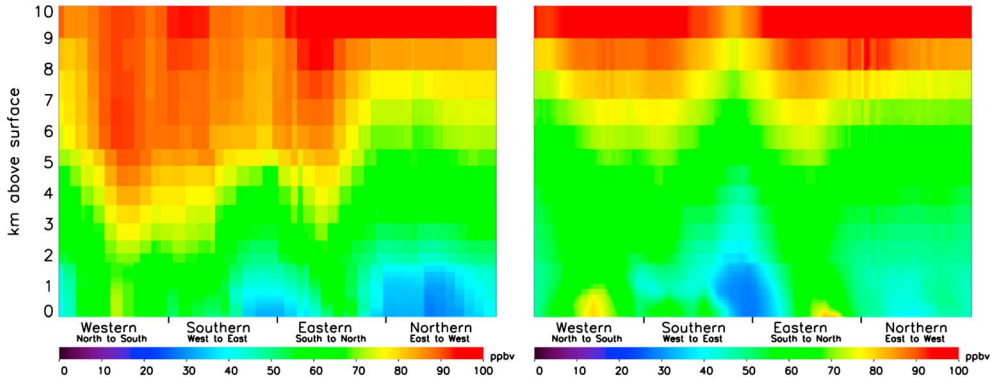

Figure 11. (left) GEOS-Chem ozone mixing ratios (ppbv) from the surface to 10 km following the model domain boundary (as shown in Figure 1) for the July 2011 mean. (right) Same as left, but now using the MOZART-4 global model.

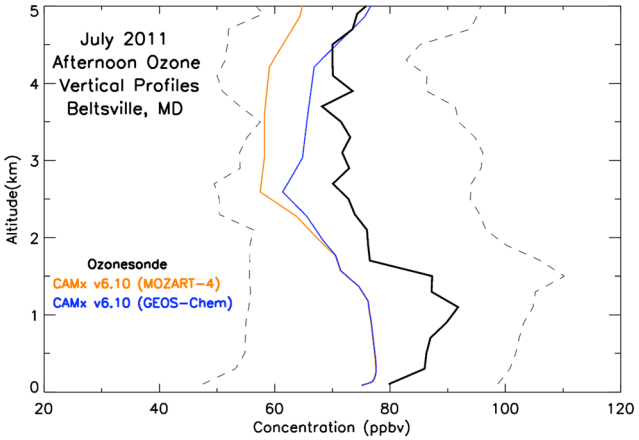

Figure 12. Mean vertical profiles of ozone (black curve) observed from the ozonesondes launched from Beltsville, MD [*Thompson et al.*, 2014], (orange curve) CAMx simulation using MOZART-4 as boundary conditions, and (blue curve) CAMx simulation using GEOS-Chem as boundary conditions at the closest model grid point.

variability improved correlation and reduced the mean bias; adding interannual variability did not improve correlation but did improve the mean bias. Boundary conditions can be essential for accurate simulation in regional air quality models [*Tang et al.*, 2007, 2009].

There are two global models commonly used to initialize the trace gases at the boundary of regional air quality models: GEOS-Chem [*Bey et al.*, 2001] and MOZART-4 [*Emmons et al.*, 2010]. Figure 11 shows mean July monthly ozone mixing ratios in GEOS-Chem and MOZART-4 along our model domain boundary. In the midtroposphere, 2–7 km above the surface (roughly 800–300 hPa), ozone is much higher in GEOS-Chem, especially at the western boundary. Mean GEOS-Chem mixing ratios in the midtroposphere often exceed 90 ppbv at the western boundary, while MOZART-4 mixing ratios average 50 ppbv. Taking a closer look, between 0 and 2 km above ground surface, there is a lot of variability between the two global models, but there is no consistent bias. Between 2 and 7 km, GEOS-Chem has mixing ratios stunningly higher than MOZART at all boundaries, but most notably at the western boundary. Above 8 km, primarily in the lower stratosphere, the mean ozone mixing ratios from MOZART and GEOS-Chem agree once again.

The different boundary initializations can significantly alter the simulation of ozone in Maryland. In Figure 12, we plot mean vertical profiles of ozone from ozonesondes [*Thompson et al.*, 2014] and from CAMx initialized with both global models. Simulation of mean near-surface ozone is quite good, within 5 ppbv, but there is a striking under estimate ($>$ 10 ppbv) of ozone between 500 and 4000 m agl by both initializations. Between 2000 and 5000 m agl, CAMx initialized with GEOS-Chem simulates uniformly greater mixing ratios than CAMx initialized with MOZART-4. We posit two explanations for the poor simulation of ozone above the surface: inadequate vertical mixing of ozone and its precursors, which has been known to be a problem [*Solazzo et al.*, 2013; *Castellanos et al.*, 2011], and/or an underestimation of ozone at the boundary.

4. Conclusions

Surface ozone in the northeastern United States is projected to decline due to reductions in anthropogenic nitrogen oxide (NO_x) and volatile organic compound (VOC) emissions driven by air quality regulations and market-based fuel switches. However, using observed values in the Baltimore-Washington metropolitan area, we find surface ozone during relatively clean summertime days (the 33rd percentile) to be rising at a rate of $+0.37 \pm 0.04$ ppb/yr. This finding comes in stark contrast to the steady decreases in total surface ozone observed during the worst air quality days. NO_x and VOC emission reductions contributed to the decreases during the worst air quality days [e.g., *Loughner et al.*, 2014], but the reasons for the increase during clean days are still unclear [*Lin et al.*, 2000; *Cooper et al.*, 2012]. We suggest that decreasing NO_x and HO_2 in rural areas and aloft plumes are causing an increase in the lifetime of ozone. This allows ozone to be transported greater distances than a decade ago.

Simulations from CAMx show the portion attributed to BC_{O3}, beyond the control of the eastern United States, will become a larger share as anthropogenic NO_x and VOC emissions in our model domain decrease. Between July 2002 and July 2018, BC_{O3} rises from 34.5% to 43.6% of the total surface ozone in Baltimore. Similar increases are seen in other metropolitan areas in the eastern United States. Not only has BC_{O3} increased by percentage but also in an absolute sense, from 26.0 to 27.2 ppbv between July 2002 and July 2018. This increase cannot be attributed to international transport, meteorological differences, or the stratosphere

because we initialize the boundary and meteorology identically in each simulation; it must be a result of the changes to the emissions within our model domain.

Two processes that are sinks for ozone: $O_3 + HO_2$ and nitrate formation are becoming less effective at removing odd oxygen; this is increasing the lifetime of ozone in the domain. The increased lifetime of ozone associated with these two sinks is +4.6% over a 16 year period and can account for the +4.6% change in BC_{O3} over the same 16 year period. The longer lifetime of ozone will increase the spatial and temporal scale of ozone pollution, which adds urgency to control ozone precursors on a regional scale especially when the standard is tightened in future years. Decreasing anthropogenic VOC and NO_x emissions in the eastern United States has had the unintentional consequence of weakening two ozone destruction pathways.

These results also point out the importance of evaluating the global models used to initialize the boundaries of regional air quality models. We show substantial variance in ozone mixing ratios between the GEOS-Chem and MOZART-4 global models; differences of >30 ppbv ozone exist in the free troposphere. This variability leads to 1–2 ppbv differences in surface ozone simulation averaged over an entire month with greater inconsistency at the surface during individual days. Regional air quality simulations must initialize boundaries with the most accurate data possible because ozone coming from the boundary is a significant and likely growing contributor to policy-relevant surface concentrations.

Acknowledgments

We thank Glenn Wolfe, Daniel Jacob, and three anonymous reviewers for their critical feedback in the preparation of this paper. We also thank Julie McDill and Susan Wierman from the Mid-Atlantic Regional Air Management Association (MARAMA) in preparation of the emissions used for the July 2011 and July 2018 model scenarios. We are also grateful for the ozonesonde data collected by Everette Joseph's research group at Howard University. The Maryland Department of the Environment (MDE) (G. Tad Aburn, Michael Woodman, and Jennifer Hains), the NASA Air Quality Applied Sciences Team (AQAST), and the NASA Modeling, Analysis, and Prediction Program all funded this research. CAMx source code has been provided by Ramboll Environ and can be freely downloaded (http://www.camx.com). Observations of surface ozone, carbon monoxide, and nitrogen dioxide have been obtained freely from the AirNow Data Management Center (http://www.airnowtech.org) and EPA Air Quality System (AQS) Data Mart (http://www.epa.gov/ttn/airs/aqsdatamart).

References

Akritidis, D., P. Zanis, E. Katragkou, M. G. Schultz, I. Tegoulias, A. Poupkou, K. Markakis, I. Pytharoulis, and T. Karacostas (2013), Evaluating the impact of chemical boundary conditions on near surface ozone in regional climate-air quality simulations over Europe, *Atmos. Res.*, *134*, 116–130, doi:10.1016/j.atmosres.2013.07.021.

Allen, D. J., K. E. Pickering, R. W. Pinder, B. H. Henderson, K. W. Appel, and A. Prados (2012), Impact of lightning-NO on eastern United States photochemistry during the summer of 2006 as determined using the CMAQ model, *Atmos. Chem. Phys.*, *12*(4), 1737–1758, doi:10.5194/acp-12-1737-2012.

Anderson, D. C., et al. (2014), Measured and modeled CO and NO_y in DISCOVER-AQ: An evaluation of emissions and chemistry over the eastern US, *Atmos. Environ.*, *96*, 78–87.

Anenberg, S. C., L. W. Horowitz, D. Q. Tong, and J. J. West (2010), An estimate of the global burden of anthropogenic ozone and fine particulate matter on premature human mortality using atmospheric modeling, *Environ. Health Perspect.*, *118*(9), 1189–1195, doi:10.1289/ehp.0901220.

Baker, K. R., C. Emery, P. Dolwick, and G. Yarwood (2015), Photochemical grid model estimates of lateral boundary contributions to ozone and particulate matter across the continental United States, *Atmos. Environ.*, *123*, 49–62.

Bell, M. L., A. McDermott, S. L. Zeger, J. M. Samet, and F. Dominici (2004), Ozone and short-term mortality in 95 US urban communities, 1987–2000, *J. Am. Med. Assoc.*, *292*(19), 2372–2378.

Bell, M. L., R. D. Peng, and F. Dominici (2006), The exposure-response curve for ozone and risk of mortality and the adequacy of current ozone regulations, *Environ. Health Perspect.*, *114*(4), 532–36.

Bey, I., D. J. Jacob, R. M. Yantosca, J. A. Logan, B. D. Field, A. M. Fiore, Q. B. Li, H. G. Y. Liu, L. J. Mickley, and M. G. Schultz (2001), Global modeling of tropospheric chemistry with assimilated meteorology: Model description and evaluation, *J. Geophys. Res.*, *106*(D19), 23,073–23,095.

Canty, T. P., L. Hembeck, T. P. Vinciguerra, D. C. Anderson, D. L. Goldberg, S. F. Carpenter, D. J. Allen, C. P. Loughner, R. J. Salawitch, and R. R. Dickerson (2015), Ozone and NO_x chemistry in the eastern US: Evaluation of CMAQ/CB05 with satellite (OMI) data, *Atmos. Chem. Phys. Discuss.*, *15*(4), 4427–4461.

Carlton, A. G., and K. R. Baker (2011), Photochemical modeling of the Ozark Isoprene Volcano: MEGAN, BEIS, and their impacts on air quality predictions, *Environ. Sci. Technol.*, *45*(10), 4438–4445.

Castellanos, P., L. T. Marufu, B. G. Doddridge, B. F. Taubman, J. J. Schwab, J. C. Hains, S. H. Ehrman, and R. R. Dickerson (2011), Ozone, oxides of nitrogen, and carbon monoxide during pollution events over the eastern United States: An evaluation of emissions and vertical mixing, *J. Geophys. Res.*, *116*, D16307, doi:10.1029/2010JD014540.

Colella, P., and P. R. Woodward (1984), The piecewise parabolic method (PPM) for gas-dynamical simulations, *J. Comput. Phys.*, *54*(1), 174–201.

Collet, S., H. Minoura, T. Kidokoro, Y. Sonoda, Y. Kinugasa, P. Karamchandani, J. Johnson, T. Shah, J. Jung, and A. DenBleyker (2014), Future year ozone source attribution modeling studies for the eastern and western United States, *J. Air Waste Manage. Assoc.*, *64*(10), 1174–1185, doi:10.1080/10962247.2014.936629.

Cooper, O. R., et al. (2010), Increasing springtime ozone mixing ratios in the free troposphere over western North America, *Nature*, *463*(7279), 344–348, doi:10.1038/nature08708.

Cooper, O. R., S.-R. Gao, D. Tarasick, T. Leblanc, and C. Sweeney (2012), Long-term ozone trends at rural ozone monitoring sites across the United States, 1990–2010, *J. Geophys. Res.*, *117*, D22307, doi:10.1029/2012JD018261.

Derwent, R. G., P. G. Simmonds, A. J. Manning, and T. G. Spain (2007), Trends over a 20-year period from 1987 to 2007 in surface ozone at the atmospheric research station, Mace Head, Ireland, *Atmos. Environ.*, *41*(39), 9091–9098, doi:10.1016/j.atmosenv.2007.08.008.

Dolwick, P., F. Akhtar, K. R. Baker, N. Possiel, H. Simon, and G. Tonnesen (2015), Comparison of background ozone estimates over the western United States based on two separate model methodologies, *Atmos. Environ.*, *109*, 282–296, doi:10.1016/j.atmosenv.2015.01.005.

Emery, C., J. Jung, N. Downey, J. Johnson, M. Jimenez, G. Yarwood, and R. Morris (2012), Regional and global modeling estimates of policy relevant background ozone over the United States, *Atmos. Environ.*, *47*, 206–217, doi:10.1016/j.atmosenv.2011.11.012.

Emmons, L. K., S. Walters, P. G. Hess, J.-F. Lamarque, G. G. Pfister, D. Fillmore, C. Granier, A. Guenther, D. Kinnison, and T. Laepple (2010), Description and evaluation of the Model for Ozone and Related chemical Tracers, version 4 (MOZART-4), *Geosci. Model Dev.*, *3*(1), 43–67.

Environmental Protection Agency (EPA) (2012), Air quality designations for the 2008 Ozone National Ambient Air Quality Standards. [Retrieved from http://www.gpo.gov/fdsys/pkg/FR-2012-05-21/pdf/2012-11618.pdf.]

Environmental Protection Agency (EPA) (2014a), National Ambient Air Quality Standards for ozone. [Retrieved June 2015 from http://www.epa.gov/airquality/ozonepollution/pdfs/20141125proposal.pdf.]
Environmental Protection Agency (EPA) (2014b), Meteorology technical support document—Meteorological model performance for annual 2011 WRF v3.4 simulation. [Retrieved June 2015 from http://www.epa.gov/ttn/scram/reports/MET_TSD_2011_final_11-26-14.pdf.]
Environmental Protection Agency (EPA) (2014c), Technical support document (TSD) preparation of emissions inventories for the version 6.0, 2011 emissions modeling platform. [Retrieved June 2015 from http://www.epa.gov/ttn/chief/emch/2011v6/outreach/2011v6_2018base_EmisMod_TSD_26feb2014.pdf.]
Environmental Protection Agency (EPA) (2014d), Modeling guidance for demonstrating attainment of air quality goals for ozone, PM2.5, and regional haze. [Retrieved June 2015 from http://www.epa.gov/ttn/scram/guidance/guide/Draft_O3-PM-RH_Modeling_Guidance-2014.pdf].
Environmental Protection Agency (EPA) (2015a), National Ambient Air Quality Standards for Ozone. [Retrieved December 2015 from https://www.gpo.gov/fdsys/pkg/FR-2015-10-26/pdf/2015-26594.pdf.]
Environmental Protection Agency (EPA) (2015b), Air quality modeling technical support document for the 2008 ozone NAAQS transport assessment. [Retrieved from http://www.epa.gov/airtransport/O3TransportAQModelingTSD.pdf.]
Fann, N., A. D. Lamson, S. C. Anenberg, K. Wesson, D. Risley, and B. J. Hubbell (2011), Estimating the national public health burden associated with exposure to ambient PM2.5 and ozone, *Risk Anal.*, *32*(1), 81–95.
Fehsenfeld, F. C., R. R. Dickerson, G. Hubler, W. T. Luke, L. J. Nunnermacker, E. J. Williams, J. M. Roberts, J. G. Calvert, C. M. Curran, and A. C. Delany (1987), A ground-based intercomparison of NO, NO_x, and NO_y measurement techniques, *J. Geophys. Res.*, *92*(12), 710–722.
Fiore, A. M., D. J. Jacob, J. A. Logan, and J. H. Yin (1998), Long-term trends in ground level ozone over the contiguous United States, 1980–1995, *J. Geophys. Res.*, *103*(D1), 1471–1480.
Fiore, A. M., J. T. Oberman, M. Y. Lin, L. Zhang, O. E. Clifton, D. J. Jacob, V. Naik, L. W. Horowitz, J. P. Pinto, and G. P. Milly (2014), Estimating North American background ozone in US surface air with two independent global models: Variability, uncertainties, and recommendations, *Atmos. Environ.*, *96*, 284–300.
Fujita, E. M., D. E. Campbell, B. Zielinska, J. C. Chow, C. E. Lindhjem, A. DenBleyker, G. A. Bishop, B. G. Schuchmann, D. H. Stedman, and D. R. Lawson (2012), Comparison of the MOVES2010a, MOBILE6.2, and EMFAC2007 mobile source emission models with on-road traffic tunnel and remote sensing measurements, *J. Air Waste Manage.*, *62*(10), 1134–1149.
Goldberg, D. L., C. P. Loughner, M. Tzortziou, J. W. Stehr, K. E. Pickering, L. T. Marufu, and R. R. Dickerson (2014), Higher surface ozone concentrations over the Chesapeake Bay than over the adjacent land: Observations and models from the DISCOVER-AQ and CBODAQ campaigns, *Atmos. Environ.*, *84*, 9–19.
Gratz, L. E., D. A. Jaffe, and J. R. Hee (2015), Causes of increasing ozone and decreasing carbon monoxide in springtime at the Mt. Bachelor Observatory from 2004 to 2013, *Atmos. Environ.*, *109*, 323–330.
Guenther, A. B., X. Jiang, C. L. Heald, T. Sakulyanontvittaya, T. Duhl, L. K. Emmons, and X. Wang (2012), The Model of Emissions of Gases and Aerosols from Nature version 2.1 (MEGAN2.1): An extended and updated framework for modeling biogenic emissions, *Geosci. Model Dev.*, *5*(6), 1471–1492, doi:10.5194/gmd-5-1471-2012.
He, H., J. W. Stehr, J. C. Hains, D. J. Krask, B. G. Doddridge, K. Y. Vinnikov, T. P. Canty, K. M. Hosley, R. J. Salawitch, and R. R. Dickerson (2013), Trends in emissions and concentrations of air pollutants in the lower troposphere in the Baltimore/Washington airshed from 1997 to 2011, *Atmos. Chem. Phys.*, *13*, 1–16.
Henderson, B. H., F. Akhtar, H. O. T. Pye, S. L. Napelenok, and W. T. Hutzell (2014), A database and tool for boundary conditions for regional air quality modeling: Description and evaluation, *Geosci. Model Dev.*, *7*(1), 339–360.
Hildebrandt-Ruiz, L., and G. Yarwood (2013), Interactions between organic aerosol and NO_y: Influence on oxidant production. Final report for AQRP project 12–012. Prepared for the Texas Air Quality Research Program.
Houyoux, M. R., and J. M. Vukovich (1999), Updates to the Sparse Matrix Operator Kernel Emissions (SMOKE) modeling system and integration with Models-3. *The Emission Inventory: Regional Strategies for the Future*, *1461*.
Hudman, R. C., N. E. Moore, A. K. Mebust, R. V. Martin, A. R. Russell, L. C. Valin, and R. C. Cohen (2012), Steps towards a mechanistic model of global soil nitric oxide emissions: Implementation and space based-constraints, *Atmos. Chem. Phys.*, *12*(16), 7779–7795.
Jacob, D. J. (2000), Heterogeneous chemistry and tropospheric ozone, *Atmos. Environ.*, *34*(12), 2131–2159.
Jacob, D. J., J. A. Logan, and P. P. Murti (1999), Effect of rising Asian emissions on surface ozone in the United States, *Geophys. Res. Lett.*, *26*(14), 2175–2178, doi:10.1029/1999GL900450.
Jaffe, D., and J. Ray (2007), Increase in surface ozone at rural sites in the western US, *Atmos. Environ.*, *41*(26), 5452–5463.
Jerrett, M., R. T. Burnett, C. A. Pope III, K. Ito, G. Thurston, D. Krewski, Y. Shi, E. Calle, and M. Thun (2009), Long-term ozone exposure and mortality, *N. Engl. J. Med.*, *360*(11), 1085–1095.
Kota, S. H., Q. Ying, and G. W. Schade (2012), MOVES vs. MOBILE6.2: Differences in emission factors and regional air quality predictions. Transportation Research Board 91st Annual Meeting (12–4438).
Lamarque, J. F., P. Hess, L. Emmons, L. Buja, W. Washington, and C. Granier (2005), Tropospheric ozone evolution between 1890 and 1990, *J. Geophys. Res.*, *110*, D18213, doi:10.1029/2012JD017723.
Langford, A. O., J. Brioude, O. R. Cooper, C. J. Senff, R. J. Alvarez II, R. M. Hardesty, B. J. Johnson, and S. J. Oltmans (2012), Stratospheric influence on surface ozone in the Los Angeles area during late spring and early summer of 2010, *J. Geophys. Res.*, *117*, D00V06, doi:10.1029/2011JD016766.
Lefohn, A. S., C. Emery, D. Shadwick, H. Wernli, J. Jung, and S. J. Oltmans (2014), Estimates of background surface ozone concentrations in the United States based on model-derived source apportionment, *Atmos. Environ.*, *84*, 275–288, doi:10.1016/j.atmosenv.2013.11.033.
Lin, C. Y. C., D. J. Jacob, J. W. Munger, and A. M. Fiore (2000), Increasing background ozone in surface air over the United States, *Geophys. Res. Lett.*, *27*(21), 3465–3468, doi:10.1029/2000GL011762.
Lin, C. Y. C., D. J. Jacob, and A. M. Fiore (2001), Trends in exceedances of the ozone air quality standard in the continental United States, 1980–1998, *Atmos. Environ.*, *35*(19), 3217–3228.
Lin, M., A. M. Fiore, O. R. Cooper, L. W. Horowitz, A. O. Langford, H. Levy II, B. J. Johnson, V. Naik, S. J. Oltmans, and C. J. Senff (2012a), Springtime high surface ozone events over the western United States: Quantifying the role of stratospheric intrusions, *J. Geophys. Res.*, *117*, D00V22, doi:10.1029/2012JD018151.
Lin, M., A. M. Fiore, L. W. Horowitz, O. R. Cooper, V. Naik, J. Holloway, B. J. Johnson, A. M. Middlebrook, S. J. Oltmans, and I. B. Pollack (2012b), Transport of Asian ozone pollution into surface air over the western United States in spring, *J. Geophys. Res.*, *117*, D00V07, doi:10.1029/2011JD016961.
Loughner, C. P., D. J. Allen, K. E. Pickering, D. L. Zhang, Y. X. Shou, and R. R. Dickerson (2011), Impact of fair-weather cumulus clouds and the Chesapeake Bay breeze on pollutant transport and transformation, *Atmos. Environ.*, *45*(24), 4060–4072, doi:10.1016/j.atmosenv.2011.04.003.
Loughner, C. P., B. Duncan, and J. Hains (2014), The benefit of historical air pollution emissions reductions during extreme heat, *Environ. Manager*, 34–38.

Martinez, M., et al. (2003), OH and HO_2 concentrations, sources, and loss rates during the southern oxidants study in Nashville, Tennessee, summer 1999, *J. Geophys. Res.*, *108*(D19), 4617, doi:10.1029/2003JD003551.
National Climate Data Center (NCDC) (2015), Quality controlled local climatological data. [Retrieved from http://www.ncdc.noaa.gov/qclcd/QCLCD.]
O'Brien, J. J. (1970), A note on the vertical structure of the eddy exchange coefficient in the planetary boundary layer, *J. Atmos. Sci.*, *27*(8), 1213–1215.
Oltmans, S. J., A. S. Lefohn, J. M. Harris, I. Galbally, H. E. Scheel, G. Bodeker, E. Brunke, H. Claude, D. Tarasick, and B. J. Johnson (2006), Long-term changes in tropospheric ozone, *Atmos. Environ.*, *40*(17), 3156–3173.
Oltmans, S. J., A. S. Lefohn, D. Shadwick, J. M. Harris, H. E. Scheel, I. Galbally, D. W. Tarasick, B. J. Johnson, E.-G. Brunke, and H. Claude (2013), Recent tropospheric ozone changes—A pattern dominated by slow or no growth, *Atmos. Environ.*, *67*, 331–351.
Paoletti, E., and W. J. Manning (2007), Toward a biologically significant and usable standard for ozone that will also protect plants, *Environ. Pollut.*, *150*(1), 85–95.
Parrish, D. D., D. B. Millet, and A. H. Goldstein (2009), Increasing ozone in marine boundary layer inflow at the west coasts of North America and Europe, *Atmos. Chem. Phys.*, *9*(4), 1303–1323.
Pouliot, G., and T. E. Pierce (2009), Integration of the Model of Emissions of Gases and Aerosols from Nature (MEGAN) into the CMAQ modeling system, presented at the 18th International Emission Inventory Conference, Baltimore, Md.
Ramboll Environ (2014), CAMx version 6.10 user's guide. [Retrieved from http://www.camx.com/files/camxusersguide_v6-10.pdf.]
Samoli, E., et al. (2006), Short-term effects of nitrogen dioxide on mortality: An analysis within the APHEA project, *Eur. Respir. J.*, *27*(6), 1129–1137.
Sandermann, H. (1996), Ozone and plant health, *Annu. Rev. Phytopathol.*, *34*, 347–366.
Sickles, J. E., and D. S. Shadwick (2015), Air quality and atmospheric deposition in the eastern US: 20 years of change, *Atmos. Chem. Phys.*, *15*(1), 173–197, doi:10.5194/acp-15-173-2015.
Simon, H., A. Reff, B. Wells, J. Xing, and N. Frank (2015), Ozone trends across the United States over a period of decreasing NO_x and VOC emissions, *Environ. Sci. Technol.*, *49*(1), 186–195.
Skamarock, W. C., J. B. Klemp, J. Dudhia, D. O. Gill, D. M. Barker, W. Wang, and J. G. Powers (2008), A description of the advanced WRF version 3, NCAR technical note NCAR/TN/u2013475+ STR.
Solazzo, E., et al. (2013), Evaluating the capability of regional-scale air quality models to capture the vertical distribution of pollutants, *Geosci. Model Dev.*, *6*(3), 791–818, doi:10.5194/gmd-6-791-2013.
Stammer, D., F. Wentz, and C. Gentemann (2003), Validation of microwave sea surface temperature measurements for climate purposes, *J. Clim.*, *16*(1), 73–87.
Stevenson, D. S., et al. (2006), Multimodel ensemble simulations of present-day and near-future tropospheric ozone, *J. Geophys. Res.*, *111*, D08301, doi:10.1029/2005JD006338.
Tang, Y., G. R. Carmichael, N. Thongboonchoo, T. Chai, L. W. Horowitz, R. B. Pierce, J. A. Al-Saadi, G. Pfister, J. M. Vukovich, and M. A. Avery (2007), Influence of lateral and top boundary conditions on regional air quality prediction: A multiscale study coupling regional and global chemical transport models, *J. Geophys. Res.*, *112*, D10S18, doi:10.1029/2006JD007515.
Tang, Y., et al. (2009), The impact of chemical lateral boundary conditions on CMAQ predictions of tropospheric ozone over the continental United States, *Environ. Fluid Mech.*, *9*(1), 43–58, doi:10.1007/s10652-008-9092-5.
Thompson, A. M., R. M. Stauffer, S. K. Miller, D. K. Martins, E. Joseph, A. J. Weinheimer, and G. S. Diskin (2014), Ozone profiles in the Baltimore-Washington region (2006–2011): Satellite comparisons and DISCOVER-AQ observations, *J. Atmos. Chem.*, *1–30*.
Trainer, M., E. Y. Hsie, S. A. McKeen, R. Tallamraju, D. D. Parrish, F. C. Fehsenfeld, and S. C. Liu (1987), Impact of natural hydrocarbons on hydroxyl and peroxy-radicals at a remote site, *J. Geophys. Res.*, *92*(D10), 11,879–11,894, doi:10.1029/JD092iD10p11879.
Val Martin, M., R. E. Honrath, R. C. Owen, G. Pfister, P. Fialho, and F. Barata (2006), Significant enhancements of nitrogen oxides, black carbon, and ozone in the North Atlantic lower free troposphere resulting from North American boreal wildfires, *J. Geophys. Res.*, *111*, D23S60, doi:10.1029/2006JD007530.
Vingarzan, R. (2004), A review of surface ozone background levels and trends, *Atmos. Environ.*, *38*(21), 3431–3442.
Vinken, G. C. M., K. F. Boersma, J. D. Maasakkers, M. Adon, and R. V. Martin (2014), Worldwide biogenic soil NO_x emissions inferred from OMI NO_2 observations, *Atmos. Chem. Phys.*, *14*(18), 10,363–10,381.
Wang, Y. H., D. J. Jacob, and J. A. Logan (1998), Global simulation of tropospheric O_3-NO_x-hydrocarbon chemistry 3. Origin of tropospheric ozone and effects of nonmethane hydrocarbons, *J. Geophys. Res.*, *103*(D9), 10,757–10,767.
Warneke, C., et al. (2010), Biogenic emission measurement and inventories determination of biogenic emissions in the eastern United States and Texas and comparison with biogenic emission inventories, *J. Geophys. Res.*, *115*, D00F18, doi:10.1029/2009JD012445.
Yarwood, G., S. Rao, M. Yocke, and G. Whitten (2005), Updates to the Carbon Bond chemical mechanism: CB05. *Final report to the US EPA*, *RT-0400675*, *8*.
Zhang, H., S. Wu, Y. Huang, and Y. Wang (2014b), Effects of stratospheric ozone recovery on photochemistry and ozone air quality in the troposphere, *Atmos. Chem. Phys.*, *14*(8), 4079–4086.
Zhang, L., et al. (2008), Transpacific transport of ozone pollution and the effect of recent Asian emission increases on air quality in North America: An integrated analysis using satellite, aircraft, ozonesonde, and surface observations, *Atmos. Chem. Phys.*, *8*(20), 6117–6136.
Zhang, L., D. J. Jacob, N. V. Downey, D. A. Wood, D. Blewitt, C. C. Carouge, A. van Donkelaar, D. B. A. Jones, L. T. Murray, and Y. Wang (2011), Improved estimate of the policy-relevant background ozone in the United States using the GEOS-Chem global model with 1/2 degrees x 2/3 degrees horizontal resolution over North America, *Atmos. Environ.*, *45*(37), 6769–6776, doi:10.1016/j.atmosenv.2011.07.054.
Zhang, L., D. J. Jacob, X. Yue, N. V. Downey, D. A. Wood, and D. Blewitt (2014a), Sources contributing to background surface ozone in the US Intermountain West, *Atmos. Chem. Phys.*, *14*(11), 5295–5309, doi:10.5194/acp-14-5295-2014.

Erratum

In the originally published version of this article, Table 1 had two errors in the 2011 column. The following have since been corrected and this version may be considered the authoritative version of record.

54.9% was changed to 42.7%

47.8% was changed to 38.8%